Preferred citation: C. Kugge, J. Daicic and I. Furó. Compressional Rheology of Model Paper Coatings. In **The science of papermaking**, *Trans. of the XIIth Fund. Res. Symp. Oxford, 2001*, (C.F. Baker, ed.), pp 1183–1202, FRC, Manchester, 2018. DOI: 10.15376/frc.2001.2.1183.

COMPRESSIONAL RHEOLOGY OF MODEL PAPER COATINGS

Christian Kugge[1], *John Daicic*[1] *and István Furó*[2]

[1]Institute for Surface Chemistry (YKI), Box 5607, SE-114 86 Stockholm, Sweden
[2]Department of Chemistry, Physical Chemistry, Royal Institute of Technology (KTH), SE-100 44 Stockholm, Sweden

ABSTRACT

The surface treatment of paper is commonly undertaken in order to improve a set of key end-use properties, including optical response and printability. These properties can be influenced, to a significant extent, by the sub-surface structure of the coating layer. The nature of coating dewatering also has strong implications for machine runnability. Thus, there is a clear need to understand in suitable detail the nature of the coating consolidation process. In this study, we have applied a novel approach to characterising the equilibrium consolidation state of calcium carbonate sediments, both with and without polymeric thickener. The aim is to provide a quantitative link between the structure of consolidated layers and their network strength, through the *compressive yield stress*, $P_y(\phi)$. A suspension, prepared at a given volume fraction of solids ϕ_0, is centrifuged to produce a consolidated particle sediment (or gel). The solidity variation of that sediment as a function of depth is then measured using one-dimensional magnetic resonance imaging (MRI), and $P_y(\phi)$ calculated directly from the volume fraction profile. The results obtained are discussed in the light of particle network structure, the effect of polymer on particle consolidation, and the relation to viscoelastic properties of the suspensions. The link to the dewatering of

coating suspensions, and structure formation in coating layers, is also considered.

INTRODUCTION

The consolidation and dewatering of paper coating suspensions is a subject of considerable importance to those involved in the surface treatment of paper. It is well known that the sub-surface structure of the coating layer has, in many applications, a direct effect on end-use behaviour, including optical properties and printability. Moreover, the dynamics of structure formation through the dewatering process has an important implication for the runnability of the coating step. It is therefore of no surprise that in recent years considerable attention has been given to obtaining a better understanding of the consolidation of paper coatings [1–10].

The traditional view of the consolidation step is that, after application, the coating suspension (including pigments, binders, thickeners, etc.) forms a filter cake through the progressive immobilisation of solid material at the interface between the substrate and the coating layer [3]. The liquid phase (water, ions, dissolved species) is chiefly absorbed into the paper substrate, or more correctly stated, is forced into the substrate through the pressure applied at the coating nip. After the formation of the filter cake, further dewatering occurs through a pressure filtration-type process, whereby the remaining liquid phase flows through the consolidated layer as this layer progressively thickens. The excess colour is (usually) scraped off, the applied layer becomes fully immobilised, and the remaining water removed through evaporation in drying units and/or the heat applied at the calendering step. Given that: (a) the consolidation process is by nature complex, involving many suspension components and (coupled) stages of development; (b) it characteristically occurs on timescales of seconds or even less; (c) it involves the consolidation of suspensions which have been delivered at very high solids content (volume fraction of solids, or solidity, ϕ, up to $\approx$0.45) and under extreme conditions of shear rate ($\approx 10^6$ s^{-1} for blade coating); it is not surprising that the development of a systematic understanding of this process from a fundamental viewpoint has proved to be a considerable challenge.

Despite these difficulties, controlled laboratory-scale studies have been attempted [1–10], sometimes being linked to results obtained from more realistic machine-based data from pilot coaters and the like. These studies have in some cases led to differences in interpretation. A number of them have focused on the nature of the filter cake [1–3,7,9], and principally whether this layer is compressible due to the presence of a concentration gradient as a

function of distance in a direction normal to the substrate surface. The resolution of this issue is of importance in modelling the dewatering process, as an incompressible layer with a uniform solidity will, at least in principle, behave differently from a compressible, non-uniform one, with respect to its resistance to flow, its internal structure (porosity and distribution of solid material), its network strength, and consequently the nature of the time evolution of consolidation.

In a valuable study, Lohmander et al. [9] investigated the pressure filtration of model suspensions with a view to resolving the solidity gradient issue. Their novel approach was to develop a pressure filtration cell for use inside a medical magnetic resonance image (MRI) device. They were thus able to measure, through this imaging technique, the solidity of the consolidated layer as a function of height within the sediment as the liquid phase was expunged through it. The suspensions consisted of monodisperse polystyrene spheres as model pigments and, in some cases, a polymer as a model for a thickener. Within the claimed resolution of their instrument, ≈0.8 mm, Lohmander et al. were able to show that a solidity gradient indeed exists, with ϕ ranging from 0.48 at the interface with the unconsolidated suspension to 0.71 at the filter base, over a filter cake height of ≈3.5 mm. Moreover, they were able to account for flow-rate data from their experiments in terms of a model for flow through compressible filter cakes. While typical coating layers are several orders of magnitude thinner than the filter cakes investigated by Lohmander et al., being typically ≈10 μm thick, the work of these authors provided an important step in the systematic characterisation of flow through consolidating coating suspensions.

Indeed, it can be said that the work of Lohmander et al. follows a tradition whereby previously semi-empirical approaches to studying flow through consolidated beds have been systematised through an analysis which involves measurement or deduction of the internal structure of the cake, and correlation to flow or mechanical properties through a detailed model of the compressional rheology of the suspension. This approach was initiated by Buscall and White [11] in the 1980s, and continued by them and co-workers [12–16], and others including Bergström [17,18] and Zukoski [19–21]. Studies of compressional rheology have led to considerable advancement of the understanding of the consolidation of particle suspensions, with applications to mineral processing, ceramics and waste-water treatment.

As stated, one of the possible approaches to studying the compressional rheology of particle suspensions is through pressure filtration, as done by Lohmander et al. [9] and others previously [14,15]. Another is to use batch centrifugation [11,16,19]. In the latter case, a particle suspension is centrifuged in order to exaggerate the effect of gravity, so that the sedimentation of

the suspension can be effected relatively rapidly and equilibrium reached. Moreover, the centrifugation method can provide a direct means of determining the *compressive yield stress* $P_y(\phi)$ of the system.

Before proceeding further, a brief discussion of $P_y(\phi)$, which is a material property of the consolidated layer, is warranted. The following is based on that presented by Landman and White in Ref. [14]. In a stable suspension, where individual particles are stabilised by colloidal interparticle forces, such as electrostatic forces, external pressures are resisted by the sum of the particle pressures p_p, which is equivalent to the osmotic pressure $\Pi(\phi)$. If the suspension is flocculated, the particles instead interact directly through contact (steric) forces and are thus able to build up a local particle pressure. As the system is consolidated, a gelation threshold, ϕ_g is reached, where, on some macroscopic length scale, each particle is in contact with one or more other particles, forming a network, or percolated, structure. This network then has an internal pressure which can resist external loads, and which may be increased through e.g. application of a pressure, or centrifugation. The network can in fact resist loads until they exceed the compressive yield stress, $P_y(\phi)$, at which point the system collapses and consolidates irreversibly. Therefore, measurement of $P_y(\phi)$ gives key rheological information regarding a consolidating system, as it indicates the strength of the network at a given solids content and also the magnitude of external forces that can be supported before irreversible collapse. Moreover, the nature of the dependence of $P_y(\phi)$ on the solidity ϕ under variations in system conditions, such as initial solidity ϕ_0, pH, ionic strength or the presence of polymeric additives, can indicate the relative role of colloidal forces and packing considerations at differing degrees of consolidation. With respect to coating colours, it is suggested that $P_y(\phi)$ data will form a useful complement to more traditional, coarser-grained empirical parameters such as the first and second critical concentrations (FCC and SCC) [5,8], and may even at the practical level provide useful information for fine-tuning, e.g. blade loadings. The main advantage is that one obtains a quantitative parameter linking local layer structure to its material properties, which in turn can be related to composition of the suspension. Furthermore, combining pressure filtration and centrifugation studies can provide detailed information regarding the link between these properties, and flow.

Returning now to the centrifugation method, we can state that it has successfully been applied to mineral particle systems previously in two distinct ways [19]. The first of these involves measuring the sediment height at different centrifugation speeds [16,19]. Clearly, this is a somewhat laborious approach. An alternative is to centrifuge to equilibrium at a given g, and then measure the solidity of the sediment as a function of height [18,19]. A

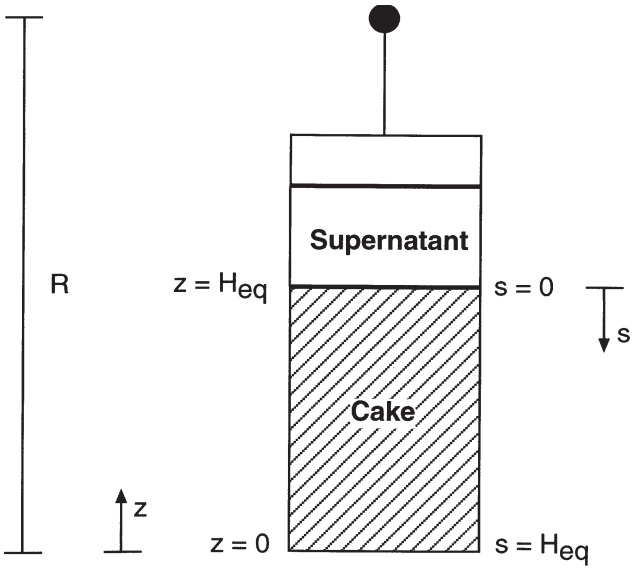

Figure 1 Sketch of centrifugation setup.

schematic diagram of a typical measurement geometry is given in Figure 1. At equilibrium, the pressure acting upon any point in the particle network is simply the cumulative weight of all particles above that point, so that [18,19]

$$P(z) = \int_{z}^{H_{eq}} \Delta\rho g(z)\phi(z)dz \tag{1}$$

where $g(z) = \omega^2 R(1 - z/R)$, z is the distance from the bottom of the column, ω is the angular frequency of the centrifuge, R is the total distance from the rotation centre to the bottom of the column, H_{eq} is the equilibrium height of the sediment, and $\Delta\rho$ is the density difference between the solid and liquid phases. As Miller et al. [19] state, the compressive yield model asserts that, at equilibrium, $P_y[\phi(z)] = P(z)$; that is, the equilibrium state is such that the centrifuge force and the particle network force balance each other. A simpler way to parametrise the integral in Equation (1) is through the substitution $s = H_{eq} - z$, so that

$$P_y[\phi(s)] = \int_0^s \Delta\rho g(s)\phi(s)ds \tag{2}$$

Thus, all that is required to obtain $P_y(\phi)$ is to perform a single centrifugation experiment to equilibrium, measure the solidity profile in the cake, and evaluate the weighted integral in Equation (2). Measurement of the solidity profile has been done previously by sectioning and weighing [19], or by scattering of γ-rays [18]. The sectioning approach removes the need for expensive instrumentation, but is a laborious and destructive method. The γ-ray scattering approach is attractive by being non-intrusive, but suffers somewhat in resolution due to beam collimation limits, which are usually of the order of several mm.

In the current study, one-dimensional (1D) magnetic resonance imaging (MRI) experiments were used as a means to determine the solidity profiles. This is similar to the approach used by Lohmander et al. [9] in their pressure filtration studies, the main difference being that a conventional NMR spectrometer with a micro-imaging probe, rather than a medical imaging instrument, has been employed, giving considerably better resolution, on the order of 0.3 mm. This, to our knowledge, is the highest imaging resolution used to date in this kind of study. NMR imaging is described in detail in Refs. [22,23]. The principle of the method is that it detects the concentration of water by ^{1}H NMR, while the mineral pigments and other species not containing ^{1}H give no NMR signal. In short, we have used a high-resolution, non-intrusive method to evaluate the compressive yield stress of model coating suspensions, over a broad range of solidities above the gelation point ϕ_g and up to high packing densities close to full immobilisation. Again, this is achieved with a single centrifugation and imaging experiment for a given system.

As the aim of this paper is to demonstrate the approach and apply it to model systems only, we restrict our study here to two cases: A ground calcium carbonate suspension (a standard coating pigment grade) dispersed by sodium polyacrylate, and a like suspension with the same solids content, but where 1 pph (against dry pigment) of a standard paper coating polymeric thickener, carboxymethylcellulose (CMC), has been added. We then discuss our results for $P_y(\phi)$ in the light of viscoelasticity data for these two systems, as well as implications for their consolidation behaviour.

EXPERIMENTAL

Materials

The pigment used is ground $CaCO_3$ (GCC), Omyalite 90 (Omya AG), with a particle size distribution of 90% < 2.5 μm as measured with a MasterSizer 2000 instrument, and a density of 2.71 g/cm^3. The thickener is sodium carboxymethylcellulose (CMC, Finn-Fix® FF10, Metsä Speciality Chemicals Oy), with a molecular weight of approximately 65 000 g/mol. Sodium polyacrylate (NaPA, Dispex N40, Allied Colloids) with a molecular weight of 3000 g/mol was used as a dispersing agent. The amount of NaPA was fixed at 0.3 pph against dry pigment.

Sample preparation

The suspensions were prepared by adding dispersing agent to the pigment suspension at a given solids content during mechanical stirring for 15 min at 500 rpm. For the thickener-containing sample, CMC was added during stirring and followed by 15 min at 500 rpm of continuous stirring after *pH* was measured and adjusted to 8.5. A final homogenous suspension was obtained by continued stirring for 60 min at 500 rpm after the solids content was measured. As a last step in the preparation, the suspensions were placed into an ultrasound bath for 10 min.

Both samples were prepared at a suspension particle solidity of $\phi_0 = 0.21$ and are labelled GCC-0 (no CMC added) and GCC-CMC (1 pph of CMC against dry pigment) respectively.

Centrifugation

A Beckman Optima™ L-90K ultracentrifuge was used with a swinging bucket SW55 Ti rotor. An amount of 1.8 g of the samples were placed into NMR-tubes (Wilmad) with a flat bottom and an internal diameter of 8.6 mm. The NMR-tubes were in turn placed into centrifugation tubes, the temperature set to 23°C, and the sample centrifuged at 2900 rpm (so that $\omega = 303.7$ rad s^{-1} corresponding to an acceleration of 9650 ms^{-2} at the base of the sediment) for 1 hr , so that equilibrium is reached. The distance from the rotation centre to the base of the suspension (inner side of base of the NMR tube) was $R = 104.6$ mm. The magnetic resonance imaging experiments were performed within 24 hr of centrifugation.

Magnetic resonance imaging (MRI)

The one-dimensional (1D) magnetic resonance imaging (MRI) experiments [22,23] were performed on a Bruker DMX200 NMR spectrometer equipped with a Bruker 10mm micro-imaging probe. The short samples contained in flat-bottom tubes were subject to a large inhomogeneity of the static magnetic field due to the macroscopic (in contrast to the microscopic one that is created around each solid particle in the sediment) discontinuity of the diamagnetic susceptibility within and around the sample. By careful shimming, this macroscopic inhomogeneity has been reduced to a value that, in the absence of imaging field gradients, provided a 250–300 Hz line width of the ^{1}H spectrum of the water in the sample.

The sample tubes were placed at the same vertical position in the probe with an accuracy of ±0.5 mm and imaged along their z-axis by 1D imaging experiments with the z gradient coil set of the probe fed by current pulses from a Bruker BAFPA-40 current amplifier. The strength of the applied imaging gradient pulse was determined by observing the 1D image of pure water filled in identical tubes up to the same height as the sediments. Two experiments with gradients of the same value but opposite directions were carried out and the gradient value for the imaging experiments was established as the minimum gradient at which the two images were, by a reasonable approximation, mirror images of each other. This minimum value was found to be approximately 8 G/cm.

The 1D imaging experiments were performed using the

$$(\alpha) - \tau - (\beta)_{\varphi} - \tau - \text{detection}\,(\varphi_R)$$

spin echo pulse sequence applied in the presence of the 8 G/cm imaging gradient pulse. At this gradient value, the images created for the ≈ 1cm high columns were 30–40 kHz wide. Consequently, the strength of the radio-frequency (rf) field created by the saddle rf coil of the probe (providing 15 μs length for a 180° pulse) was insufficient to homogeneously excite the full spectrum for a conventional $90 - \tau - 180°$ spin echo [22]. Hence, the echo experiment was performed with pulses shorter ($\alpha = 25°$ and $\beta = 50°$) than the conventional values. Distortions introduced by this choice of pulse angles were eliminated [24] by cycling the pulse (φ) and receiver (φ_R) phases according to the Exorcycle scheme [25]. The short pulse angles also reduced the signal-to-noise ratio which was partly compensated for by collecting 256 scans. The recycling time was set to at least $5T_1$ (the longitudinal relaxation time T_1 of water in the sediments, measured by a spatially resolved inversion recovery experiment, was 150–200 ms). A typical 1D image of a sediment

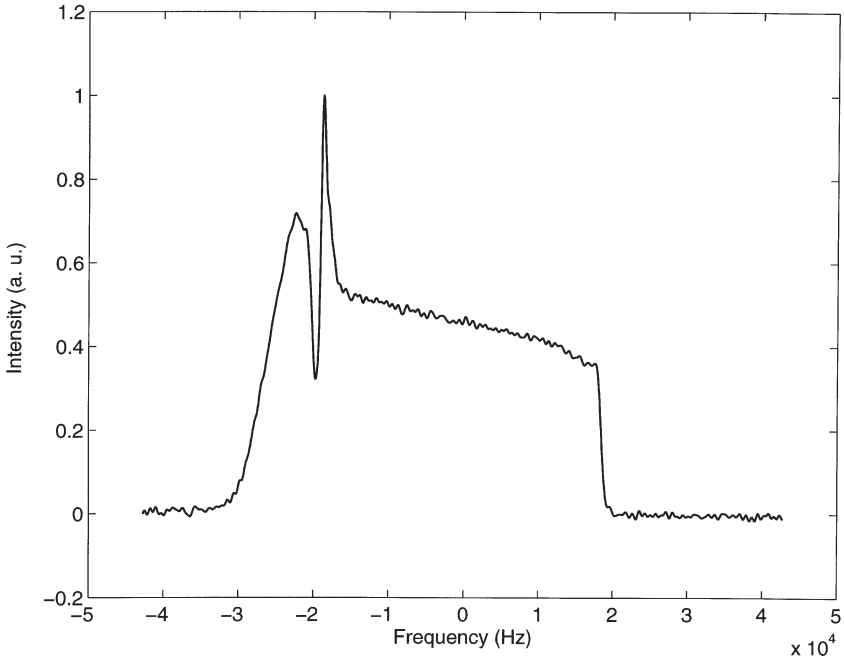

Figure 2 1D image of a sediment sample.

sample is shown in Figure 2. The peaks at the left edge correspond to the image of bulk water on the sample top shaped by the meniscus and the large magnetic field inhomogeneity in that region.

There are several factors that define the spatial resolution of the obtained information. The ≤300 Hz linewidth (see above) inherently limits the resolution to

$$(10\ \text{mm}) \times (300\ \text{Hz})/(30\ 000\ \text{Hz})$$

that is about 100 μm. This limit could be somewhat lowered, at the cost of signal-to-noise ratio, by applying a stronger gradient. The second factor is the inhomogeneity of the applied z gradient in the x–y plane that spreads the spectral intensity from the same spatial slice along the NMR frequency axis. This effect can be quantified from the right edge of the profile in Figure 2 that

corresponds to the bottom of the sample. The width of this edge (partly contributed by the imperfection of the bottom plate of the sample tube) is around 1 kHz , corresponding to ≈300 μm. This value of edge imperfection includes a contribution from the magnetic field inhomogeneity. Hence, we can conclude that a conservative estimate of the spatial resolution of the image is ≤300 μm.

The inhomogeneity of the z gradient along the z axis is the main reason of not having a perfectly flat profile even in the images of the bulk water samples (not shown). This artefact can be partly compensated for by normalising the obtained sediment image intensities with the intensities in the water image. This normalisation requires the comparison of intensities at the same distance from the sample bottom that can be easily obtained using the right edges of the respective images as references. However, the ±0.5 mm inaccuracy of the sample position may still cause a few percentage errors in the intensities that is not compensated. This should be kept in mind when comparing results for different samples. The results for the solidity profiles are obtained by integrating the spectral intensities for 400 μm wide slices along the z direction for two sediment samples and comparing the obtained figures to the respective intensities yielded by a bulk water sample. Hence, the average volume fraction of solid particles within the selected slices can be plotted on a vertical scale against depth within the sediment.

Viscoelasticity measurements

Oscillatory shear measurements were performed using a controlled stress Physica UDS 200 rheometer, an instrument with a broad detectable torque range. A solvent trap filled with water was used to avoid evaporation. The rheometer was equipped with a concentric cylinder geometry cell, with a sand-blasted bob. The viscoelastic measurements were performed directly after sample preparation to avoid effects of sedimentation, and without an applied shear history, in order to study undisturbed suspensions at low deformations. The strain sweeps (0.01–100%) were done with a constant frequency of 1 Hz.

RESULTS AND DISCUSSION

Solidity profiles

After centrifugation, the equilibrium height of the cakes was measured to be $H_{eq} = 9.5 \pm 0.3$ mm for the GCC-0 sample, and $H_{eq} = 9.0 \pm 0.3$ mm for the GCC-CMC sample. We use these values to scale the depth in the cake as

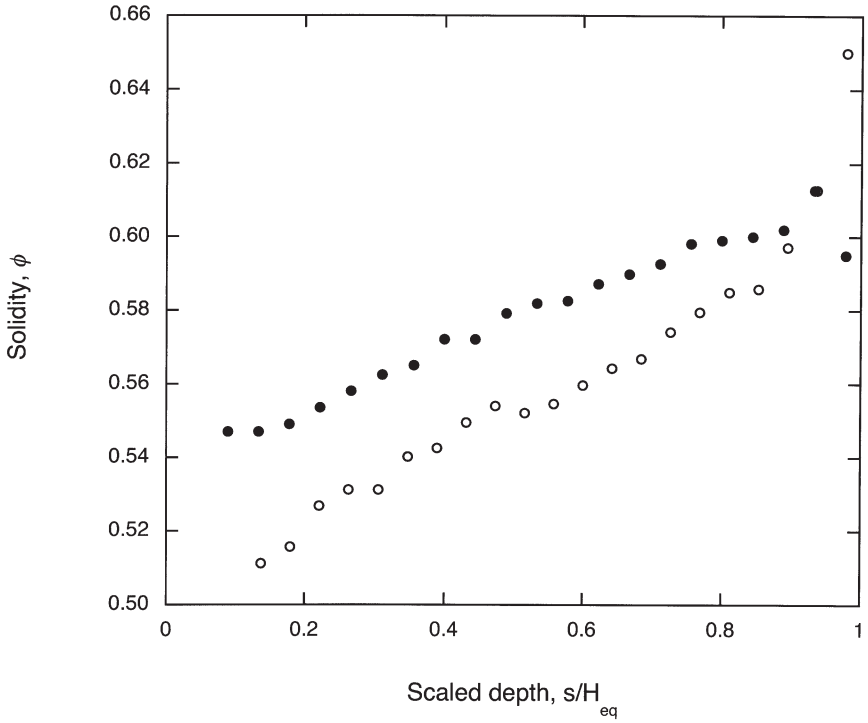

Figure 3 Solidity profiles for the GCC-0 sample (unfilled circles) and the GCC-CMC sample (filled circles) obtained from the 1D MRI measurements.

s/H_{eq}, and then present, in Figure 3, the solidity profiles obtained from the MRI measurements, against this scaled depth.

The first point to note is that, in keeping with the findings of Lohmander et al. [9], the sediment cakes of both samples showed a distinct solidity gradient. Note also that while both samples were prepared at an initial solidity of $\phi_0 = 0.21$, the filter cakes themselves showed much higher solidity, in the range of $\phi \approx 0.5$ to 0.65. It should be noted however that some information has been lost regarding the solidity near the supernatant-cake interface, due to the large magnetic field inhomogeneity there (see Figure 2), so that the first measurement of the solidity is for $s/H_{eq} \approx 0.1$. However, the fact that these slurries can be prepared as stable or at least partly flocculated suspensions up to $\phi_0 \approx 0.50$ indicates that, at equilibrium, a compressed layer of with $\phi \approx 0.21$ is unlikely to have formed near the supernatant-cake interface, and linear

extrapolation of points at lower s values to $s \to 0$ should give a reasonable indication of the solidity near that interface. In any case, we have no indication that, even for an initial solidity of $\phi_0 = 0.21$, a network capable of supporting external loads is formed until consolidation has proceeded to $\phi \approx 0.5$, and this is in keeping with our former understanding of coating colour consolidation. This extrapolation procedure provides an estimate of the gelation point of each sample: $\phi_g \approx 0.49$ for GCC-0, and $\phi_g \approx 0.545$ for GCC-CMC.

We focus now on the differences in solidity profile between the two samples introduced by the presence of 1 pph of polymer in the sample GCC-CMC. The solidity profile for the GCC-CMC showed a gentler slope over a narrower range of solidities than the CMC-free GCC-0 sample. The effect of polymer is to produce a more homogeneous cake. This is also in keeping with the results of Lohmander et al. [9] in their pressure filtration experiments. Of particular note is the fact that as $s/H_{\mathrm{eq}} \to 1$, there is a clear drop in the solidity of the GCC-CMC sample, while ϕ continues to increase towards close packing for the GCC-0 sample. While admittedly this difference relies on one data point, it is a clear trend that lies within experimental confidence limits. Any suggested cause given for this difference would be speculative at this point, but one guess may be that there is an inhomogeneous distribution of polymer in the cake, causing an anomalously large reduction in particle solidity at the bottom of the cylinder. Indeed, means of determining the polymer distribution in the sediment is an interesting subject for future studies, and the NMR method provides possibilities by which to investigate this, for example through molecular labelling techniques.

For the GCC-0 sample, it is interesting to note that the highest measured solidity of the cake is $\phi = 0.65$ at $s/H_{\mathrm{eq}} = 0.98$. In a separate study [26], we have investigated the steady-shear viscosity of the GCC-0 system over a broad range of ϕ_0 values. The relative plastic viscosity η_{rpl} was measured as a function of ϕ_0 from $\phi_0 = 0.0034$ to 0.52 using a combination of capillary viscometry and steady-shear rheometry. The data was then fitted to the Krieger–Dougherty model [27]

$$\eta_{\mathrm{rpl}}(\phi_0) = \left(1 - \frac{\phi_0}{\phi_m}\right)^{-[\eta]\phi_m} \tag{3}$$

where $[\eta]$ is the intrinsic viscosity, or shape factor, and ϕ_m is the maximum packing fraction. The Krieger–Dougherty model is a mean-field approximation to the solidity dependence of the viscosity, and ϕ_m represents in effect an extrapolation to maximum packing. A non-linear fit to the data from the GCC-0 system using the MATHEMATICA® package produced a value of

$\phi_m = 0.708 \pm 0.005$. Comparing this to the data obtained from the centrifugation measurement, one could deduce that an even tighter packing of the particles may be possible in the bottom 300 μm of the cake, and the steep gradient in the profile seems to support this. (The fact that $\phi = 0.64$ and $\phi = 0.74$ correspond to, respectively, close random packing and face centred cubic packing for monodisperse spheres is noted, but the latter case more as a point of curiosity value, given that the sample we are using contains non-spherical particles in a somewhat polydisperse distribution.)

Compressive yield stress

The procedure for evaluating the compressive yield stress was as follows: The solidity profile data was fitted with a polynomial, such that the R^2 value was better than 0.99. Thus the error so introduced is within the experimental confidence limits of a few percent. The exception was the point for the GCC-CMC system at $s/H_{eq} = 0.98$ and $\phi = 0.595$ at the bottom of the column, where the solidity has dipped, as discussed above. The motivations for removing this point from the analysis were: (a) a good polynomial fit could not be obtained if it were included; (b) more fundamentally, such a dip in the solidity at the base of the cylinder is not predicted in the model suggested by equation (2), and must lie outside its scope. However, that model can still be used to evaluate $P_y(\phi)$ for all other points in the data set for the GCC-CMC system. Furthermore, the fits were designed to be consistent with a linear extrapolation of s values to $s \to 0$ by first fitting the lowest three s values linearly, extrapolating to $s \to 0$, adding this point to the data set and then performing the polynomial fit to this augmented data set. (The extrapolated ϕ-values are however not included in calculations of $P_y(\phi)$ values themselves, but rather as a means of obtaining a more reliable fit to the original data set.) It must however be acknowledged that there is a degree of approximation introduced by this procedure, and it would be much preferred if the technique could be improved to directly measure the solidity at the lowest s values. In the light of this approximation procedure, differences in the compressive yield stress between the two samples should be seen in relative, rather than absolute, terms.

These polynomial fits were then integrated according to equation (2) using the MATHEMATICA® package, and values for P_y so obtained paired with corresponding ϕ values. That these ϕ values were produced from the polynomial fits rather than taken from the data set itself was seen as a more self-consistent procedure, but admittedly introduced a degree of artificial smoothening to the calculated values of $P_y(\phi)$. In any case, the differences between the two systems were large enough to not be affected to any

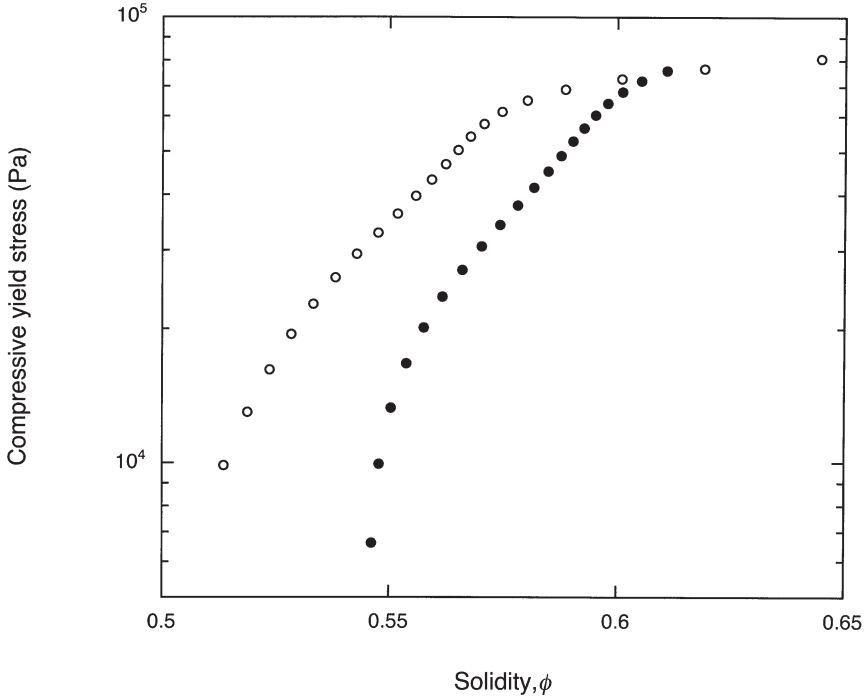

Figure 4 Compressive yield stress, $P_y(\phi)$, for the GCC-0 sample (unfilled circles) and the GCC-CMC sample (filled circles).

significant degree by this "smoothening" procedure. The results are presented in Figure 4.

The difference between the two samples is clear: Over most of the solidity range, $P_y(\phi)$ is significantly lower at comparable values ϕ for the GCC-CMC system than for its thickener-free counterpart GCC-0. The introduction of polymer has produced a network which is *weaker* with respect to its resistance to compressive loads, and this leads to the more uniform solidity profile seen in Figure 3 here, and previously reported by Lohmander et al. [9]. At higher solids, the data sets appear to begin to merge, as they should: As the particles are packed more tightly, differences in structure arising from effects which have a range longer than the particle size, including polymeric forces such as steric stabilisation and bridging (adsorbed polymer) and depletion forces (non-adsorbed polymer) [28], should begin to be minimised. In this way, the

$P_y(\phi)$ curve indicates the evolution between the colloidal-dominated and packing dominated regimes in the consolidation process.

Another interesting feature of the result for GCC-0 is that $P_y(\phi)$ does not yet appear to reach the asymptote of $P_y(\phi) \to \infty$ at a volume fraction where further packing is not possible, indicating that a very dense layer could be present at the very base of the column, and is not accessible within our resolution limits. In any case, the curves at least partially show the characteristic "S" shape seen in other systems [18,19,21].

An important question arises as to the underlying cause of the difference in the compressive yield stress of the two systems. Three competing hypotheses are proposed:

1. If CMC were to strongly adsorb to the pigment, polymer-induced particle bridging would occur, reducing the mobility of particles and thus hindering their ability to build optimally-packed networks to resist external loads. One would expect that $P_y(\phi)$ might be lower for such a system than for a thickener-free analogue, but only if bridging between whole flocs does not lead to an overall stronger network.
2. If CMC were to moderately adsorb to the pigment, there would be a significant steric stabilising effect. The effective particle radius would be larger than the bare particle radius; moreover the polymer would hinder optimal arrangement of particles into network structures that can resist external loads. Again, one would expect that $P_y(\phi)$ is lower for such a system than for the one without CMC, at least until the polymer layers have been maximally compressed.
3. If CMC is non-adsorbing or very weakly adsorbing, it may lead to the formation of flocs through depletion flocculation. Then, the consolidation process involves two facets: Rearrangement of aggregates, and consolidation within individual aggregates. This would also lead to a reduction in $P_y(\phi)$, as we will soon discuss.

Let us first however consider the possibilities for mechanisms 1 and 2 above. These rely on the adsorption of polymer on the pigment. What little data is available indicates that the adsorption of CMC on GCC is very weak, particularly in the presence of NaPA. Sjöberg et al. [29] have shown that the adsorbed amount of CMC on calcium carbonate pigments at 30% solids in the presence of stabilising NaPA is no greater than ≈ 0.04 mg/m^2 in a range of CMC dosages of 0–0.5 pph, way too low for either bridging or steric stabilisation to take effect. We thus have good reason to believe that CMC adsorbs only very weakly in the GCC-CMC system, and can thus effectively rule out hypotheses 1 and 2.

This leaves us with the third suggestion, that the system GCC-CMC

contains flocculated structures, due to a depletion effect, before centrifugation is commenced, and that the first consolidation step involves packing of the flocs, and the second rearrangement within the floc structures. Channell et al. [21] have recently discussed the implications of microstructure for the compressive yield stress, and have even developed a semi-empirical model for this. Reasonably, these authors state that the compressive yield stress is related to the number of interparticle bonds as

$$P_y(\phi) = \left(\frac{\text{energy}}{\text{bonds}}\right)\left(\frac{\text{bonds}}{\text{volume}}\right) f(\phi) \approx \varepsilon \frac{\phi}{\xi^3} f(\phi), \tag{4}$$

where $f(\phi)$ is related to the connectivity of the structure, ε is the average bond energy, and ξ is a characteristic size of the bond unit. Thus, it is already evident that if there are flocculated structures present, increasing the value of ξ, $P_y(\phi)$ will be reduced. At some critical solidity, ϕ_c, the flocs themselves will begin to be compressed, and this should correspond to the volume fraction of particles within the flocs. Above this solidity, flocculated and unflocculated systems that are otherwise equivalent should have the same $P_y(\phi)$ curves. Channell et al. [21] take this model further, by producing an explicit expression for $P_y(\phi)$ that takes into account the two-step nature of the consolidation process, and they find good qualitative agreement with their data from measurements on alumina suspensions. However, we were unable to successfully fit their expression to our data, although this issue will be returned to in the near future. It is nonetheless interesting to note that the trends seen in $P_y(\phi)$ by Channell et al. when flocculation is introduced into alumina suspensions are qualitatively similar to that which we observe when CMC is added to a GCC system.

What can be deduced from our data is that for this system, $\phi_c \approx 0.6$, which indicates that the polymer-induced flocs contain a high volume fraction of particles, and that colloidal forces are having an effect on structure in this system during consolidation, even at relatively high solidities.

Comparison to viscoelasticity measurements

Comparing with measurements of the storage modulus on these systems serves two purposes. The first is to compare the compressive response of the system to more familiar oscillatory shear data, and the second is to seek support for the notion that flocs are present in the thickener-containing system, and cause a general decrease in $P_y(\phi)$ in comparison to the thickener-free system over most of the solidity range.

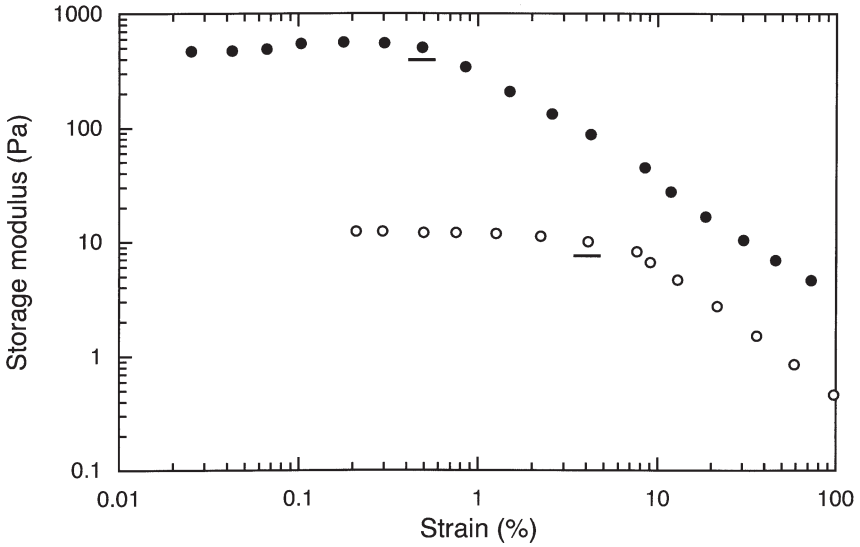

Figure 5 Storage modulus, G', for the GCC-0 sample (unfilled circles) and the GCC-CMC sample (filled circles), in a strain sweep at frequency 1 Hz. Note that $\phi_0 = 0.44$. The termination of the linear viscoelastic region is marked in both cases.

We begin by presenting, in Figure 5, the measured storage moduli, G', for both systems as a function of strain at a frequency of 1 Hz . These were measured on systems below the gel point (as they must be), with $\phi_0 = 0.44$, the idea being that if evidence for flocs is observed at this solidity, they should also be present as the gel point is approached and surpassed.

Clearly, the system containing polymer has a higher storage modulus, and this is an effect due in part simply to the presence of polymer in the continuous phase. However, the large increase in elasticity cannot be explained totally as a background effect; the polymer has caused an overall increase in the rigidity of the system. An interesting parameter is the critical strain γ_c [28], which delineates the termination of the linear viscoelastic regime with increasing strain, and these points are marked in Figure 5. Note that this value is very different for the GCC-0 ($\gamma_c \approx 4.10\%$) and GCC-CMC ($\gamma_c \approx 0.49\%$) systems. In systems containing particles at high solids content, a smaller value of γ_c indicates a higher degree of flocculation, as the system becomes more brittle: It is more elastic, but cannot be deformed to the same degree without fracturing [28]. This provides an independent indication that

the introduction of polymer has resulted in an increased degree of flocculation in the system.

The fact that the CMC-containing system is more elastic than the thickener-free system, while generally having a lower compressive yield stress, deserves comment. As stated, the link between these two properties seems very likely to be the induction of flocculation by the polymer. The higher elasticity of the suspension is due in some part to the internal strength of the flocs. In contrast, $P_y(\phi)$ is reduced due to the fact that consolidation involves the packing of large units, until a critical solidity is reached, where the internal volume fraction of flocs, and the overall solidity, are the same.

CONCLUDING REMARKS

The aim of the current study was to demonstrate that the centrifugation method can give useful information regarding the consolidation of model coating suspensions, and provide a quantitive characterisation of the compressibility of the consolidated layers through the compressive yield stress. We have shown how the addition of a standard thickener affects structure formation of the pigment network, and suggested that a likely mechanism is through a depletion-type flocculation. This was supported by data from viscoelastic measurements.

The method presented here shows promise as a means by which to characterise coating suspensions. Clearly, much can be done in terms of system variation, addition of binders being an obvious next step, or perhaps the choice of a highly adsorbing polymer to further investigate the role of floc formation in consolidation. Combination with pressure filtration studies is also of interest.

There are also technical issues that require further development. These include optimisation of the imaging procedure to better access the region near the cake-supernatant interface, and an explicit consideration of effects such as wall stresses. Nonetheless, the early indication is that the approach shows promise as an aid to reaching a better understanding of the complex process of coating colour consolidation.

ACKNOWLEDGEMENTS

We thank the Jacob Wallenberg Foundation, the Lars-Erik Thunholm Foundation for the Promotion of Scientific Research, the Knowledge Foundation (KK-stiftelsen), the Institute for Research and Competence Holding AB

(IRECO), and the Swedish Natural Science Research Council (NFR) for financial support. Lennart Bergström, Fredrik Tiberg and Leif Eriksson are thanked for interesting discussions.

REFERENCES

1. Engström, G., "Development of the Solids Content in the Coating Layer between Application and Blade", *Wochbl. Papierfabr.*, **114**: 195–199, 1986.
2. Eklund, D.E. and Salminen, P.J., "The Dewatering of Coating Colours", *Tappi J.*, 69, 116–119, 1986.
3. Letzelter, P. and Eklund, D. "Coating Color Dewatering in Blade Coaters. Part 1: Mathematical Model and the Influence of Color Parameters", *Tappi J.*, **76**: 63–68, 1993.
4. Letzelter, P. and Eklund, D., "Coating Color Dewatering in Blade Coaters. Part 2: The Influence of Machine Configuration", *Tappi J.*, **76**: 93–98, 1993.
5. Young, T.S., Pivonka, D.E., Weyer, L.G. and Ching, B., "A Study of Coating Water Loss and Immobilization Under Dynamic Conditions", *Tappi J.*, **76**: 71–82, 1993.
6. Eriksson, U. and Rigdahl, M., "Dewatering of Coating Colours Containing CMC or Starch", *J. Pulp Paper Sci.*, **20**: J333–J337, 1994.
7. Salminen, P.J., Roper, J., Pollock, M. and Yohannes, C., "Determining the Dynamic Water Retention Contribution of Various Cobinders and Thickeners", *Tappi Coating Conf. Proceedings*. Tappi Press, Atlanta, 227–286, 1995.
8. Stanislawska, A. and Lepoutre, P., "Consolidation of Pigmented Coatings: Development of Porous Structure", *Tappi Coating Conf. Proceedings*. Tappi Press, Atlanta, 67–77, 1995.
9. Lohmander, S., Martinez, M., Li, T.-Q., Lason, L. and Rigdahl, M., "Dewatering of Coating Dispersions – Model Experiments and Analysis", *Tappi Advanced Coating Fundam. Symp. Proceedings*. Tappi Press, Atlanta: 43–58, 1999.
10. Bernard, H., Morin, V., Rueff, M. and Mondjian, P., "A Study of the Migration of Liquids into Paper in View of Modelling Coating Colour Dewatering", *Scientific and Technical Advances in Paper Coatings Proceedings*. Pira International, Surrey, 2000.
11. Buscall, R. and White, L.R., "The Consolidation of Concentrated Suspensions", *J. Chem. Soc. Faraday Trans*. **1**(83), 873–891, 1987.
12. Buscall, R., Mills, P.D.A., Goodwin, J.W. and Lawson, D.W., "Scaling Behaviour of the Rheology of Aggregate Networks Formed from Colloidal Particles", *J. Chem. Soc. Faraday Trans.* **1**(84): 4249–4260, 1988.
13. Landman, K.A., Sirakoff, C. and White, L.R., "Dewatering of Flocculated Suspensions by Pressure Filtration", *Phys. Fluids* **A**(3): 1495–1509, 1991.
14. Landman, K.A. and White, L.R., "Solid/Liquid Separation of Flocculated Suspensions", *Adv. Colloid Interface Sci.*, **51**: 175–246, 1994.

15. Landman, K.A., White, L.R. and Eberl, M., "Pressure Filtration of Flocculated Suspensions", *AIChE J.*, **41**: 1687–1700, 1995.
16. Green, M.D., Eberl M. and Landman, K.A., "Compressive Yield Stress of Flocculated Suspensions: Determination via Experiment", *AIChE J.*, **42**: 2308–2318, 1996.
17. Bergström, L., "Sedimentation of Flocculated Alumina Suspensions: γ-Ray Measurements and Comparison with Model Predictions", *J. Chem. Soc. Faraday Trans.*, **88**: 3201–3211, 1992.
18. Bergström, L., Schilling, C.H. and Aksay, I.A., "Consolidation Behaviour of Flocculated Alumina Suspensions", *J. Am. Ceram. Soc.*, **75**: 3305–3314, 1992.
19. Miller, K.T., Melant, R.M. and Zukoski, C.F., "Comparison of the Compressive Yield Response of Aggregated Suspensions: Pressure Filtration, Centrifugation and Osmotic Consolidation", *J. Am. Ceram. Soc.,* **79**: 2545–2556, 1996.
20. Channell, G.M. and Zukoski, C.F., "Shear and Compressive Rheology of Aggregated Alumina Suspensions", *AIChE J.*, **43**: 1700–1708, 1997.
21. Channell, G.M., Miller, K.T. and Zukoski, C.F., "Effects of Microstructure on the Compressive Yield Stress", *AIChE J.*, **46**: 72–78, 2000.
22. Ernst, R.R., Bodenhausen, G. and Wokaun, A., "Principles of Nuclear Magnetic Resonance in One and Two Dimensions". Clarendon Press, Oxford: 1987.
23. Price, W.S., "NMR Imaging", *Ann. Rep. NMR Spectrosc.*, (ed. G.H. Webb). Academic Press, London: 139–216, 1998.
24. Rance, M. and Byrd, R.A., "Obtaining High-Fidelity Spin-1/2 Powder Spectra in Anisotropic Media: Phase-Cycled Hahn Echo Spectroscopy", *J. Magn. Reson.*, **52**: 221–240, 1983.
25. Bodenhausen, G., Freeman, R. and Turner, D.L., "Suppression of Artefacts in Two-Dimensional J Spectroscopy", *J. Magn. Reson.*, **27**: 511–514, 1977.
26. Kugge, C., Daicic, J., and Ström, G., "Shear Response of Concentrated Calcium Carbonate Suspensions", manuscript to be submitted, 2001.
27. Krieger, I.M. and Dougherty, T.J., "A Mechanism for Non-Newtonian Flow in Suspensions of Rigid Spheres", *Trans. Soc. Rheology*, **3**: 137–152, 1959.
28. Larson, R.G., *The Structure and Rheology of Complex Fluids*. Oxford University Press, Oxford: 1999.
29. Sjöberg, M., Larsson, A. and Sjöström, E., "Adsorption of Water-Soluble Polymers and Surfactants on Pigments", *Institute for Surface Chemistry Report B425*. Stockholm, 1996.

Transcription of Discussion

COMPRESSIONAL RHEOLOGY OF MODEL PAPER COATINGS

Christian Kugge[1], *John Daicic*[1] *and István Furó*[2]

[1]Institute for Surface Chemistry
[2]Department of Chemistry, Royal Institute of Technology

Theo van de Ven Paprican, McGill University

If the flocculation effect is due to depletion, that is usually a reversible phenomenon. If you dilute the system, the flocs should redisperse. Is that what you find?

John Daicic

We haven't done that measurement yet, but that is a very relevant question, I think that should be done.

Patrice Mangin Centre Technique du Papier

I would like to suggest that you put some of your conclusions into Volume 3, because they are not clear in your original paper – the flocculation division you should maybe add them at the end.

John Daicic

Yes I will be glad to do that. (*Ed. Note in subsequent correspondence it was agreed that the conclusions in the original paper were clear.*)